Waves in Random Media 2 (1992) 209–224. Printed in the UK

Simulation of a Kolmogorov phase screen

R G Lane, A Glindemann and J C Dainty
Blackett Laboratory, Imperial College, London SW7 2BZ, UK

Received 14 August 1991, in final form 27 February 1992

Abstract. Two new methods for modelling Kolmogorov phase fluctuations over a finite aperture are described. The first method relies on the incorporation of subharmonics in order to model accurately the low frequencies of the Kolmogorov spectrum. The second method provides a less accurate, but much faster method for simulating the Kolmogorov spectrum by using a midpoint displacement algorithm used in computer graphics.

1. Background

The simulation of atmospherically distorted wavefronts is an important tool for studying light propagation and imaging. The work in this paper is motivated by the need to develop efficient and effective methods of imaging astronomical objects through the turbulent atmosphere. Although the true test of any imaging algorithm is always provided by actual data, a good simulation is needed to be able to test different algorithms both in a controlled manner and under a wide variety of conditions. This paper outlines new methods for simulating the effects of static atmospheric turbulence, which is an essential component of any atmospheric imaging simulation.

The starting point for nearly all analyses of atmospheric turbulence has been the assumption that atmospheric turbulence follows a Kolmogorov spectrum and has a phase that is statistically uniform over the interval $-\pi$ to π. The fluctuations induced by the turbulence then cause a distortion of both the magnitude and phase of the wavefront incident on the atmosphere. In practice the phase distortion has considerably more effect on the quality of images formed from light passing through the turbulence than those effects due to the magnitude distortion. In many situations, an adequate approximation is a single phase screen located at the entrance pupil of the optical system, although this can not account for non-isoplanatic effects [1].

A typical short exposure image formed by viewing a point source through turbulence does not consist of a single diffraction pattern with a diameter fixed by the diffraction limit of the telescope, but rather the image consists of a number of superimposed speckles distributed over a diameter determined by the severity of the turbulence. Each individual bright speckle has a diameter given approximately by the diffraction limit of the telescope. It is important that in addition to the production of a speckled distortion of the image, the simulated turbulence should also shift the centroid of the image formed. This effect of centroid motion is primarily due to the low frequencies in the Kolmogorov spectrum, which are often not modelled well in conventional FFT procedures.

Whilst it has been proposed that the centroid motion can be compensated after the generation of the speckles, this is not the only part of the information present

0959-7174/92/030209+16$04.50

in the low frequencies. Another difficulty with this approach is that when simulating time-evolving turbulence it is not obvious how to synchronize the centroid movement with the time evolution of the speckles.

2. Notation

We use the notation $p(\boldsymbol{r})$, where $\boldsymbol{r} = (x, y)$, to represent the two-dimensional phase screen in the aperture of the telescope. The phase screen is related to its spectrum by the Fourier transform pair [4]

$$P(\boldsymbol{k}) = \int_{-\infty}^{+\infty} \int_{-\infty}^{+\infty} p(\boldsymbol{r}) \exp\left(-\mathrm{i}2\pi(\boldsymbol{r} \cdot \boldsymbol{k})\right) \mathrm{d}\boldsymbol{r} \tag{1}$$

and

$$p(\boldsymbol{r}) = \int_{-\infty}^{+\infty} \int_{-\infty}^{+\infty} P(\boldsymbol{k}) \exp\left(\mathrm{i}2\pi(\boldsymbol{k} \cdot \boldsymbol{r})\right) \mathrm{d}\boldsymbol{k} \tag{2}$$

where $P(\boldsymbol{k})$ is the spectrum of the phase fluctuations.

Ideal Kolmogorov turbulence is both infinite in extent and infinite in detail. It has the unusual property that, provided certain scaling criteria are met, it 'looks' the same at whatever scale it is viewed. This is in contrast to most conventional mathematical functions which become smooth when viewed in sufficient detail. In reality true atmospheric turbulence only approaches this behaviour over the inertial range

$$L_0 > |\boldsymbol{r}| > l_0 \tag{3}$$

where L_0 is the outer scale of turbulence and could be between 2 and 100 metres or more, whilst l_0 is the inner scale and can be in the range of millimetres, although the exact values of these parameters are uncertain. The purpose of this paper is to provide simple methods for modelling turbulence over a wide range of these parameters.

One important property of the phase screens which should be generated by assuming a pure Kolmogorov spectrum is that they are not stationary, i.e. $\langle p(\boldsymbol{r})^2 \rangle$ increases without limit as $|\boldsymbol{r}| \to \infty$. It is however possible to define the phase structure function

$$D_p(|\boldsymbol{r}|) = \left\langle \left(p(\boldsymbol{r}') - p(\boldsymbol{r}' + \boldsymbol{r})\right)^2 \right\rangle \tag{4}$$

$$= 6.88(|\boldsymbol{r}|/r_0)^{5/3} \tag{5}$$

where r_0 is the Fried parameter [2] and $\langle\ \rangle$ denotes the expectation over the ensemble. It is important to note that the structure function is solely dependent on $\boldsymbol{r}$ and r_0.

One can also calculate the Wiener spectrum of the phase fluctuations

$$\Phi(\boldsymbol{k}) = 0.023 r_0^{-5/3} |\boldsymbol{k}|^{-11/3} \tag{6}$$

from the phase structure function using

$$D_p(|\boldsymbol{r}|) = 2 \int \Phi(\boldsymbol{k})[1 - \cos(2\pi \boldsymbol{k} \cdot \boldsymbol{r})] \, \mathrm{d}\boldsymbol{k} \tag{7}$$

as shown by Noll [3].

Examination of (6) shows a fundamental problem with the modelling of Kolmogorov turbulence, namely that the power in the idealized turbulence becomes infinite as $|k| \to 0$. In spite of this, the phase structure function equation (5) does show that the phase fluctuations between any two points on a finite aperture are bounded, and hence the relative phase shift across the aperture can, in principle, be modelled exactly.

In this paper we choose to analyse and simulate on a square aperture which is both mathematically and computationally convenient. The two-dimensional aperture we use is defined by

$$A(x,y) = \begin{cases} 1.0 & \text{for } |x| < D/2 \text{ and } |y| < D/2 \\ 0.0 & \text{otherwise} \end{cases} \tag{8}$$

with a Fourier transform given by

$$S(k,l) = D^2 \operatorname{sinc}(kD) \operatorname{sinc}(lD) \tag{9}$$

where

$$\operatorname{sinc}(q) = \frac{\sin(\pi q)}{\pi q}. \tag{10}$$

This in no way limits the practicality of the algorithm, since the aperture of simulation can be made a sufficient size to accommodate any shape of practical aperture.

3. Sampled representations

In conventional spectral analysis, a phase screen over a finite aperture such as (8) would be completely defined by samples of its spectrum on a rectangular grid [4] spaced by $1/D$. A difficulty with this approach becomes apparent when one considers the effects of changing the size D of the phase screen simulated. As noted by Roddier [5] it is convenient to scale the resulting phase screen values by $(D/r_0)^{5/3}$ to simulate a larger aperture. Thus in order to effectively double the size of the aperture, one need only scale a phase screen obtained for the smaller aperture by $2^{5/3}$.

In a conventional Fourier transform pair, this doubling of the size of the aperture could also be effected by increasing the sampling rate of the power spectrum. In the case of equation (6) this increased sampling does not alter the shape of the sampled spectrum, but is equivalent to scaling the values of the original samples by a factor of $2^{11/3}$ in contrast to the correct value of $2^{5/3}$ obtained from consideration of the phase structure function. This rather peculiar behaviour is a direct consequence of the fractal nature of a power law spectrum [6].

In practice the actual sampled approximation to the Kolmogorov power spectrum is given by [7]

$$\Phi(i,j) = 0.023\,(2D/r_0)^{5/3}\,(i^2 + j^2)^{-11/3} \tag{11}$$

where i and j are the sample indices. Note that the variation of the sample amplitude is solely a function of D/r_0. A typical two-dimensional phase screen obtained using

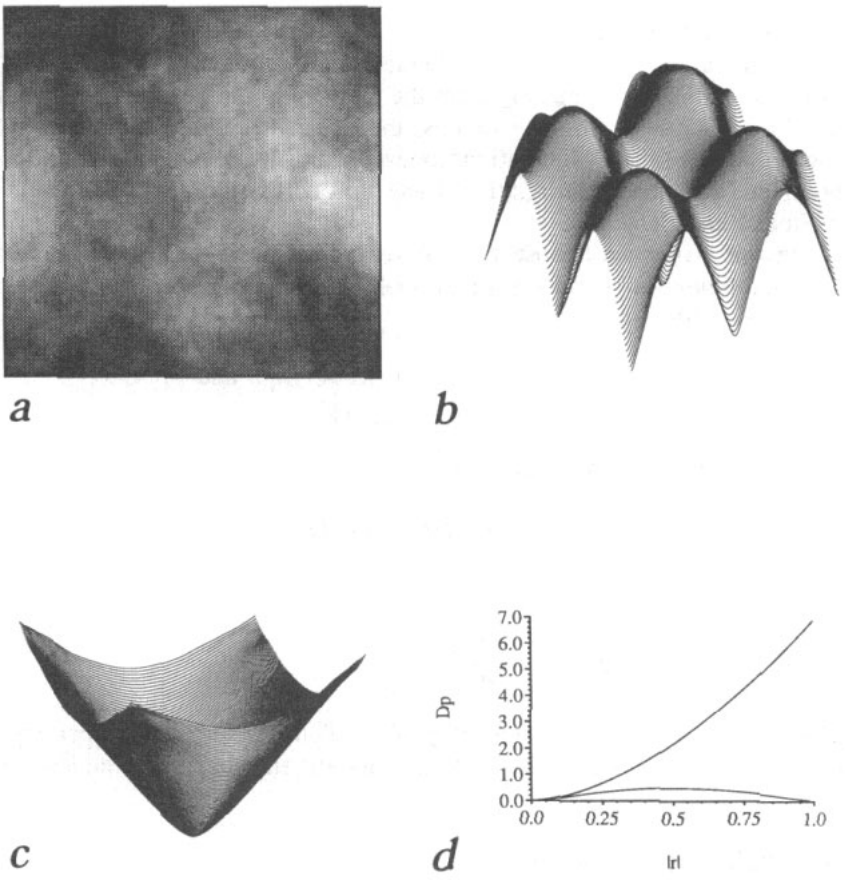

Figure 1. Phase screen approximations produced by sampling the Kolmogorov spectrum directly. (*a*) A typical phase screen produced by sampling the Kolmogorov spectrum directly. Note that the phase screen is periodic and does not appear to have any apparent overall slope. (*b*) The two-dimensional phase structure function produced from an ensemble of phase screens. (*c*) The ideal phase structure function computed from equation (5). (*d*) Sections through (*a*) and (*b*). The upper line is the ideal and the lower the approximated phase structure functions.

this approximation is shown in figure 1(*a*) and the corresponding two-dimensional phase structure function computed from an ensemble of phase screens is shown in figure 1(*b*).

There remains a further difficulty which must be overcome when using equation (11) to approximate a true Kolmogorov phase screen. It is apparent from inspection of figures 1(*a*) and 1(*b*) that the phase screen, and also the phase structure function, obtained from using this algorithm are periodic which is unlike the ideal phase structure function shown in figure 1(*c*). Figure 1(*d*) also shows one-dimensional slices through the two-dimensional phase structure of both the ideal and the crude spectral approximation afforded by equation (11). The difference between the ideal and the approximation is readily apparent.

The process of sampling means that the effect of any frequencies with a period greater than the size of the aperture, i.e. those which would correspond to either i or j being smaller than 1, are not represented. Figure 2(*a*) shows the effect of a sine

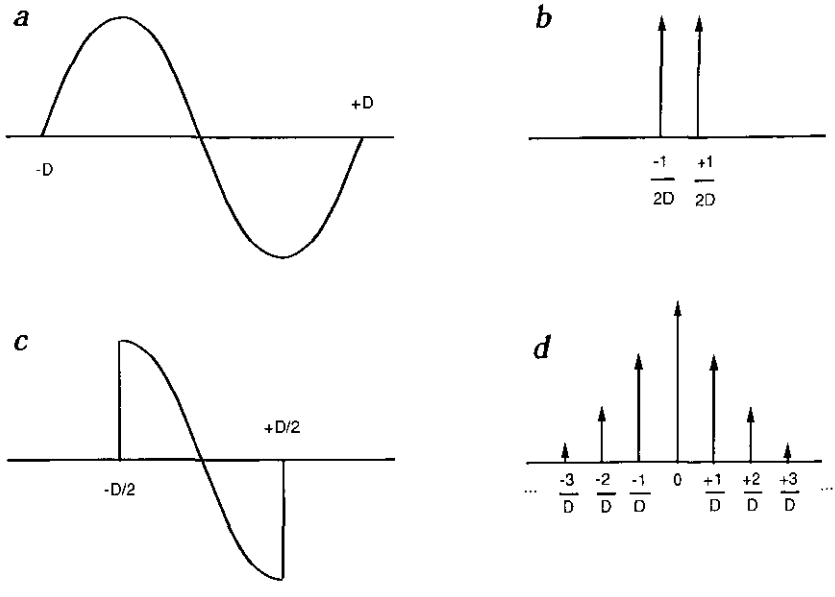

Figure 2. The effect of subharmonics on the apprent spectrum. (*a*) A sine wave with a period double the telescope aperture D. (*b*) The power spectrum of (*a*). (*c*) The observed portion of (*a*) within the telescope aperture. (*d*) A schematic showing the spectral leakage caused by (*a*).

wave which has a period twice the width of a one-dimensional aperture. The power spectrum of this true sine wave is the pair of delta functions shown in figure 2(*b*). When viewed only within the aperture (figure 2(*c*)) the sine wave can be modelled approximately by a constant slope. Since a slope in the overall wavefront corresponds to a translation of the image formed by the instrument, it is readily apparent why the absence of these lower frequencies in a simulation results in an inadequate simulation of the motion of the image formed by the instrument. It is still possible to take the Fourier transform of the truncated sine wave, and by doing so one obtains a series of harmonics spaced at $1/D$ as shown schematically in figure 2(*d*). These harmonics are not independent phasors, but are obtained by convolving the original spectrum of the sine wave with the Fourier transform of the the aperture and then resampling.

Essentially what is required is still to generate the sampled form of the Kolmogorov spectrum, except this should be done after it has been convolved with the Fourier transform of the aperture. Sampling at this stage incorporates the effects of frequencies with a period greater than the aperture.

In order to demonstrate the effects of lower frequencies, one-dimensional turbulence was simulated using equation (11) over an inertial range of $l_0 = 1\,\mathrm{mm}$ to $L_0 = 50\,\mathrm{m}$. One would expect that near perfect simulation of the turbulence would require at least $L_0/l_0 = 50\,000$ linearly spaced samples. This is because L_0 determines the required size of the aperture and l_0 the size of the finest structures present.

In the simulation the number of samples used was $2^{17} = 131\,072$, which was sufficient to exactly model the turbulence over the entire inertial range. Each sample was set equal to a circular complex Gaussian random field with real and imaginary parts having a variance equal to 1.0. The complex random field was then scaled by

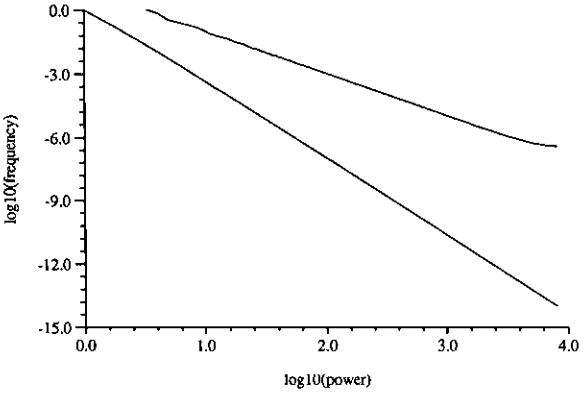

Figure 3. A comparison of the true Kolmogorov spectrum (lower line) and that computed over a finite aperture on a log–log scale. Note the lower slope is $-11/3$ as expected, whilst the upper curve slope is only -2.

the square root of the sampled power spectrum given in equation (11). The result was Fourier transformed and the real and imaginary parts extracted to form two independent phase screens. The average of the power spectrum of 100 phase screens and all 131 072 samples exhibits the expected $|\boldsymbol{k}|^{-11/3}$ variation and is shown by the lower curve in figure 3. If, however, only a subset of 16 384 samples from each phase screen is used to compute the power spectrum the spectrum decays as $|\boldsymbol{k}|^{-2}$ and is shown by the upper curve in figure 3.

Because the power spectrum of equation (6) becomes very narrow at the origin, almost in effect a delta function, the convolution of this function with the Fourier transform of the aperture results in a contribution to the higher frequencies which decays approximately as $|\boldsymbol{k}|^{-2}$, which is the rate of decay of the Fourier transform of the aperture. Because this decay is slower than the $|\boldsymbol{k}|^{-11/3}$ of the original Kolmogorov phase spectrum, the phase spectrum computed from a finite aperture should also decay approximately as $|\boldsymbol{k}|^{-2}$. The effect is identical to the familiar concept of spectral leakage in signal processing [8].

4. The fractal nature of a Kolmogorov phase screen

One of the important properties of Kolmogorov phase screens, namely that they look similar regardless of the scale they are viewed, has been one of the fundamental bases of the relatively new field of fractal geometry [6]. This property, known as self-similarity, is a direct consequence of the power spectrum of the phase fluctuations and the structure function being described by a power law.

For example, it is has already been noted that changing the size of the aperture, i.e. either enlarging or reducing the aperture by a factor α, has no effect on the shape of the phase structure function

$$D_\phi(\alpha|\boldsymbol{r}|) = \alpha^{5/3} D_\phi(|\boldsymbol{r}|). \tag{12}$$

This implies that, apart from a constant scale factor, the size of the aperture does not affect the statistics used to generate the phase screen apart from a constant scale factor. Thus when this scale factor is removed, for example by automatic scaling to fill the available grey scales on a display device, the phase screens 'appear' the same.

It is important to emphasize the difference between this behaviour and the behaviour of a conventional stochastic process. In the latter the correlation length is fixed and the appearance of the image is no longer independent of scale. In particular, a conventional stochastic process has a defined correlation length. When the size of the aperture is much below the correlation length the process appears very smooth. When the aperture is much larger than the effective correlation length the process appears completely random, since the correlated details are too small to be noticed.

5. Existing simulation techniques

If a conventional FFT based simulation is to be accurate, the number of points in the simulation depends on L_0 rather than the size of the aperture. Unfortunately, when performing two-dimensional simulations where $D \ll L_0$, this leads to a very large number of samples. For example, in the original paper by McGlamery [9] the turbulence was simulated over an area sixteen times greater than the aperture. The much improved phase structure function, when compared to the Kolmogorov ideal, is shown in figure 4, but since the computational time to compute a phase screen is approximately proportional to its area, it is achieved at more than sixteen times the computational cost.

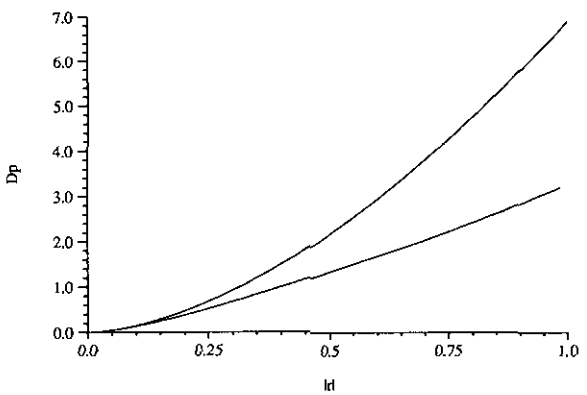

Figure 4. The improvement to the structure function obtained by only using part of the phase screen. In this case, only the centre $1/4 \times 1/4$ of the computed phase screen is used ($1/16$ of the total area). This yields a significant improvement to the approximated phase structure function but at 16 times the computational cost.

Another practical approach, suggested by Shaklan [7] is to use a phase screen with an area of only four times the size of the wanted aperture, extract the central portion of the phase screen, and then move the centroid of the resultant speckle pattern according to the formula given by Roddier [1]. Whilst this yields a much improved approximation, it does not take into account all the information present at the lower frequencies.

A completely different approach, based on Zernike polynomials, has recently been proposed by Roddier [5]. Although this approach does reproduce Kolmogorov turbulence accurately it is restricted to a circular aperture. This can be disadvantageous

if one wishes to simulate the effects of turbulence moving across the front of a telescope, since in this case a phase screen defined on rectangular cartesian coordinates is significantly more convenient. It is also open to debate whether the approach described in Roddier [5] is computationally superior to a Fourier approach since the time taken to perform an $N \times N$ Fourier transform is given by $N^2 \log_2 N^2$. In the method which uses the summation of Zernike polynomials, the computational load is proportional to αN^2, where α is the number of Zernike polynomials considered. For a 512×512 phase screen α would need to be less than 81 for the Zernike polynomial method to be faster, whereas Roddier [5] suggests the use of about 400 Zernike polynomials.

6. New approaches

In this section we describe two new approaches for simulating an ensemble of phase screens with the desired Kolmogorov spectrum. The first relies on the addition of subharmonics of the aperture and gives a very accurate phase structure function. The second relies on a variant of the random mid-point displacement algorithm, gives a good approximation to the Kolmogorov spectrum and is very fast to compute.

6.1. Addition of subharmonics

In the last section it was noted that in Kolmogorov turbulence, frequencies with periods greater than the telescope aperture still have a substantial effect on the phase screen. A simple technique for modelling the effects of these lower frequencies is to generate additional random frequencies and add their effects to the simple sampled frequencies given by equation (11).

The major difficulty is how to include the extra samples in the simulation at a level commensurate with the samples obtained by equation (11). The discrete Fourier transform

$$f_m = \sum_{n=0}^{N-1} F_n \exp(j2\pi mn/N) \tag{13}$$

uses each sample to approximate the continuous Fourier transform over one sample width by a single value, and assigns each sample equal weight as they represent an equal region in the Fourier spectrum. Near the origin in Fourier space, however, the spectrum is changing so rapidly that the single sample at the origin does not adequately model the Fourier integral. It is possible, however, to replace the single sample at the origin by nine subsamples at $(-1/3,-1/3)$, $(-1/3,0)$, $(-1/3,1/3)$, $(0,-1/3)$ etc. These samples represent only $1/9$ of the area of a conventional sample and so must be weighted by a factor of $1/9$ when they are included in the sampled approximation to the Fourier integral. We call these frequencies, which have a period greater than the aperture, subharmonics of the aperture, and the set of these eight additional samples we call the first subharmonic set.

The remaining area around $(0,0)$ can be further subdivided into patches at frequencies $(1/9,0)$, $(1/9,1/9)$ etc with a respective weighting factor of $1/9^2$ as shown in figure 5. These additional samples we call the second subharmonic set. The process is repeated, generating further subharmonic sets until the desired outer

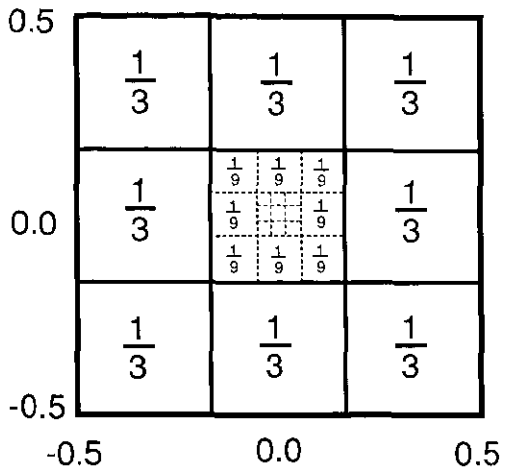

Figure 5. An enlargement of the sample at the origin of Fourier space. The area is subdivided into smaller and smaller subharmonic samples. Each is assigned a weighting proportional to the area in Fourier space.

scale of turbulence is reached. In our calculations we went down to $1/3^5$, the fifth subharmonic set, thus realizing an outer scale of turbulence 3^5 times larger than the diameter of the telescope aperture; thus the single sample at the origin is replaced by $(8+8+8+8+9) = 41$ samples.

It is not possible to use the FFT algorithm on the resultant sample set to estimate the phase screen directly because the spacing is no longer regular. It is possible, as shown in figure 2, to calculate how a sine wave contributes to the regularly spaced samples spaced at the Nyquist sampling interval. The Fourier transform of a sine wave with a period length equal to the size of the discrete array (figure 2(*a*)) results in two sinc functions with their maxima at pixel 1 and -1 (figure 2(*b*)) and having zeros coinciding with all pixel values $(\ldots,-3,-2,0,2,3,\ldots)$. If, however, the period of the sine wave is larger than the array size (figure 2(*c*)), the maxima of the sinc functions lie between pixel 0 and 1 and between 0 and -1 respectively and the function values are no longer zero on the other pixels (figure 2(*d*)). Hence each Nyquist sample of the spectrum is generated by

$$\begin{aligned} P_{\text{conv}}(k,l) &= \sqrt{0.023}\,(2D/r_0)^{5/6}\,|(k,l)|^{-11/6}\exp\bigl(\mathrm{i}\psi(k,l)\bigr) \\ P_{\text{sub}}(k,l) &= \sqrt{0.023}\,(2D/r_0)^{5/6}\,\operatorname{sinc}\bigl(\pi(k-k_s)\bigr)\operatorname{sinc}\bigl(\pi(l-l_s)\bigr) \\ &\quad \times W(k_s,l_s)|(k_s,l_s)|^{-11/6}\exp\bigl(\mathrm{i}\psi(k_s,l_s)\bigr) \\ P(k,l) &= P_{\text{conv}}(k,l) + P_{\text{sub}}(k,l) \end{aligned} \tag{14}$$

where (k,l) is the vector coordinate of the discrete array and $W(k_s,l_s)$ is the weighting factor associated with the subharmonic (k_s,l_s). The complex function $\exp\bigl(\mathrm{i}\psi(k,l)\bigr)$ provides a random, uniformly distributed phase in the spectrum and hence the random fluctuations in the phase screen. The phase screen can then be obtained by a simple Fourier transform using equation (2).

The addition of the subharmonics does, however, create a ringing phenomenon associated with the irregularly spaced samples at the edges of the phase screen. Its effects on the speckle images can be eliminated by generating the phase screen over an area twice that of the aperture and using only the central section to generate the phase screen.

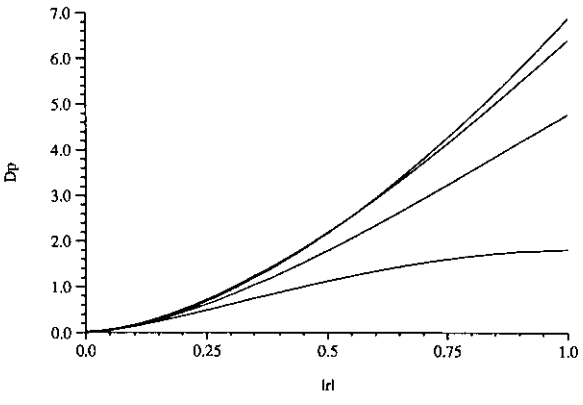

Figure 6. The improved approximation to the phase structure function yielded by the addition of subharmonics. The top curve is the ideal phase structure function. The next three curves display the effect of using one, three and five subharmonics and demonstrate that five sets of subharmonics result in a phase function very close to the ideal.

Figure 6 shows a section through the phase structure function phase screens for both the ideal and the simulation calculated with the addition of an increasing number of subharmonics. It is readily apparent that as more and more subharmonics are added, the phase structure function approaches the ideal shown by the upper line in figure 6.

This method of modelling Kolmogorov turbulence yields a wave structure function very close to the ideal function given by equation (2). Using the effect of spectral leakage there is no longer a limit to lower spatial frequencies and hence the linear shift of the speckle pattern due to low frequencies can be modelled in full agreement with the Kolmogorov spectrum. With this method one is completely free to adjust the inner and outer scale of turbulence in the simulation to the experimental data of these two numbers.

The computer time required for a single 64×64 phase screen takes 28 seconds on a SUN Sparcstation 1. Each additional subharmonic set takes about 3 seconds for a 128×128 screen. Thus a phase screen with five subharmonic sets takes 42 seconds. This compares very favourably with the 175 seconds required to compute a 256×256 phase screen and select the inner 64×64 samples.

6.2. Random mid-point displacement

The random mid-point displacement algorithm has mainly found application in the computer generation of artificial landscapes, where it results in more natural landscapes than generated by other means. The algorithm is based on making a coarsely sampled approximation to the fractal surface and then the subsequent refinement of successively smaller and smaller localized regions. The algorithm has a varied history [6] and has recently been used for computer animation [11].

The basic algorithm is most easily understood when generating a spectrum in one dimension with a power law given by

$$\Psi_b(k) = 1/k^2 \tag{15}$$

which is the spectrum of Brownian motion. Brownian motion has many features in common with Kolmogorov turbulence, and is also described in terms of its structure

function

$$D_b(\rho) = |\rho| \tag{16}$$

where D_b is used to indicate the structure function of Brownian motion.

Brownian motion has the property of independent increments, i.e. it can be formed from the integration of white noise. Since there is no correlation between different points in the random process the simulation algorithm thus starts with two independent Gaussian random variables, g_0 and g_1 with a variance equal to σ^2. Thus assuming the points g_0 and g_1 are unit length apart,

$$D_b(1) = \langle (g_0 - g_1)^2 \rangle \tag{17}$$

$$= 2\sigma^2 . \tag{18}$$

The algorithm relies on a process of successive subdivision in order to increase the resolution of the Brownian motion. A new point is formed midway between the two existing points by a process of linear interpolation and the addition of an independent random variable d_1 with a variance given by Δ^2. The variance Δ^2 is chosen so that

$$\left\langle \left(g_0 - \frac{g_0 + g_1}{2} - d_1\right)^2 \right\rangle = \sigma^2 . \tag{19}$$

Since g_0, g_1 and d_1 are all independent it is apparent that $\Delta^2 = \sigma^2/2$. The process is then iterated to produce more samples of the Brownian motion, as shown in figure 7.

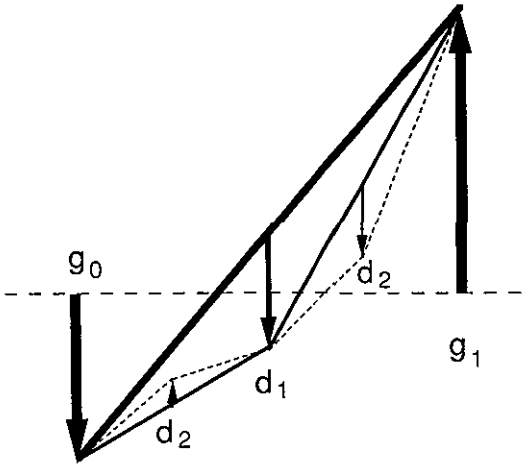

Figure 7. The midpoint displacement algorithm in one-dimension. The existing points are interpolated and a random displacement added. The procedure is then repeated until the desired number of samples are obtained.

This approach breaks down when the exponent of the power spectrum is not 2, since there is now a correlation between the random variables which must be considered when computing the required displacement [10]. Initial investigations using

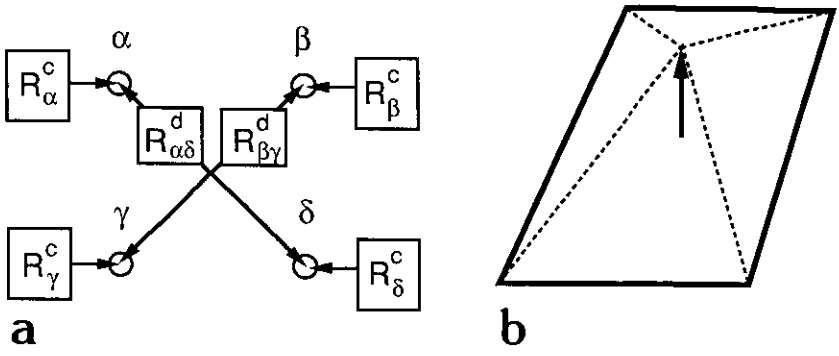

Figure 8. A two-dimensional mid-point displacement algorithm. (*a*) The four starting samples are generated from six random variables. The two diagonal terms $R_{\alpha\delta}$ and $R_{\beta\gamma}$ are needed to ensure that structure function is larger between diagonally opposite and adjacent corners. (*b*) The procedure of interpolation and displacement in two dimensions.

the computer algorithms of Fournier *et al* [11] given in Peitgen [6] failed to produce phase screens with acceptable structure functions or speckle transfer functions.

In order to simulate Kolmogorov turbulence in two-dimensions the following improved procedure was implemented. Figure 8 shows four samples denoted by α, β, γ and δ. The value of these points is given by

$$\alpha = R^c_\alpha + 0.5R^d_{\alpha\delta} \tag{20}$$

$$\beta = R^c_\beta + 0.5R^d_{\beta\gamma} \tag{21}$$

$$\gamma = R^c_\gamma - 0.5R^d_{\beta\gamma} \tag{22}$$

$$\delta = R^c_\delta - 0.5R^d_{\alpha\delta} \tag{23}$$

where R^c and R^d indicate Gaussian random variables of variance σ_c^2 and σ_d^2 respectively, and the suffixes are used to denote which of the samples are affected. Thus $R^d_{\alpha\delta}$ affects sample α and sample δ.

It is apparent that if these four samples are in fact samples from two-dimensional Kolmogorov turbulence then they must have a relationship given by (5)

$$2\sigma_c^2 + \frac{\sigma_d^2}{2} = 6.88\left(\frac{D}{r_0}\right)^{5/3} \tag{24}$$

and

$$2\sigma_c^2 + \sigma_d^2 = 6.88\left(\frac{\sqrt{2}D}{r_0}\right)^{5/3}. \tag{25}$$

It is convenient at this stage to set $D/r_0 = 1.0$ and subsequently scale the resultant phase screen by $(D/r_0)^{5/6}$. Thus the four original starting points of the phase screen are samples from Kolmogorov turbulence with $D/r_0 = 1.0$, unlike the algorithm given in Peitgen [6] which used four uncorrelated Gaussian random variables, regardless of the power spectrum that was being simulated.

It is convenient to define $(\hat{r})$ to be the distance between two adjacent samples on the sampling grid. As in the case of the one-dimensional algorithm a new point

m is formed by linear interpolation and the addition of a random displacement ϵ, although the interpolation is now between four points

$$m = \frac{\alpha + \beta + \gamma + \delta}{4} + \epsilon . \tag{26}$$

The expected value of $\langle(\alpha - m)^2\rangle$ computed from equations (20)–(23) is equal to $3.252(\hat{r})^{5/3} + \sigma_\epsilon^2$, whereas that predicted from the phase structure function is $3.861(\hat{r})^{5/3} = 6.88(\hat{r}/\sqrt{2})^{5/3}$. The variance of the displacement ϵ is thus given by $0.6091(\hat{r})^{5/3}$, compared with the value used in the algorithm given by Peitgen of $3.861(\hat{r})^{5/3}$, which takes no account of the correlation of the corner samples. Thus as the sampling grid becomes finer the variance of the random displacement is also reduced. Figure 8(*b*) shows schematically the displacement of the interpolated point in two-dimensions.

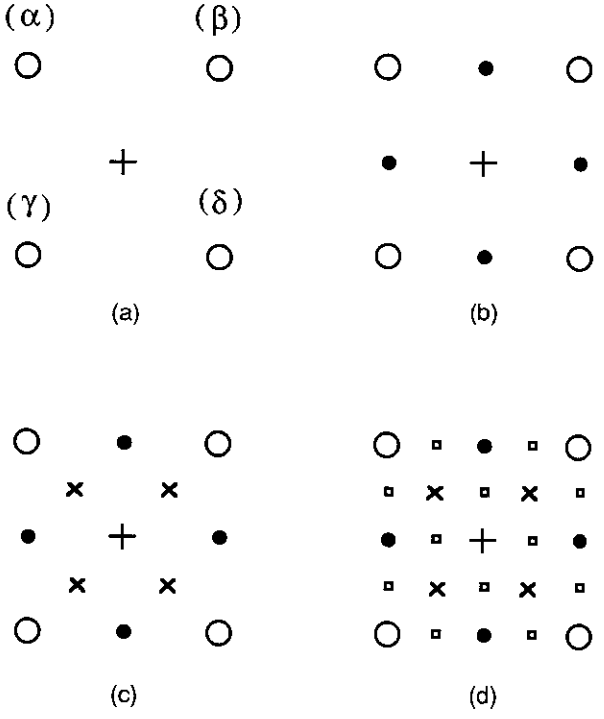

Figure 9. The interpolation sequence of a two-dimensional mid-point displacement algorithm. (*a*) The four starting samples α, β, γ and δ are used to produce the central sample. (*b*) The five samples are then used to create the samples marked by filled in dots to produce a 3 x 3 grid. (*c*) and (*d*) The stages in producing a 5 x 5 grid from a 3 x 3 grid.

Figure 9 shows how the interpolation proceeds to form an array with an arbitrary number of samples. The open circles in figure 9(*a*) are the four starting samples (marked α, β, γ and δ). They are interpolated and a random displacement added to form the sample marked by a cross. The next interpolations are formed by linearly interpolating between the corner points and again adding the random displacements, a procedure which results in the sampling grid shown in figure 9(*b*). The interpolation

between the samples on the edge requires an algorithm similar to the one-dimensional algorithm. Hence on the left edge

$$m_{\text{edge}} = \frac{\alpha + \beta}{2} + \eta \tag{27}$$

where η is a Gaussian random variable with a variance equal to $0.4471(\delta r)^{5/3}$. The next stage of interpolation and displacement forms the samples marked with a cross in figure 9(*c*). Figure 9(*d*) shows another cycle of the procedure to produce the samples marked with an open square and a 5×5 sampling grid. The interpolation/displacement procedure can be repeated until the desired number of samples is obtained [6].

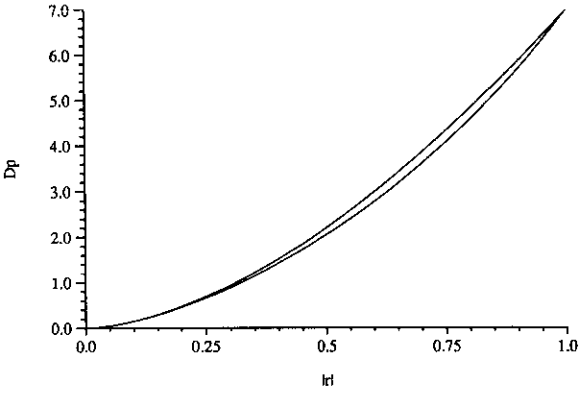

Figure 10. The fractal approximation to the phase structure function.

The procedure yields a good approximation to the phase structure function as shown in figure 10. Four typical speckle images produced by this procedure are shown in figure 11; the large displacements of the speckle centroids should be noted. It should also be noted that whilst this procedure yields a good approximation to the phase structure function, the approximation is not perfect. This is because, as noted by Mandelbrot [10], the relationship between two different interpolated points does not necessarily have the exact phase structure function. This discrepancy could be reduced by introducing a correlation between adjacent interpolated points, instead of simply using random displacements. This would, however, reduce the simplicity without significantly improving the quality of speckle simulation.

The main advantage of this technique is its speed with the number of operations being proportional to N^2. This yields a dramatic improvement in speed over all existing techniques, requiring only 0.7 seconds for a 64 x 64 array on a SUN Sparcstation 1 computer.

7. Conclusions

This paper presents two new methods for simulating a Kolmogorov phase screen. Both methods overcome the inadequate modelling of the low frequencies of the overall wavefront encountered when using conventional FFT based methods. The mid-point displacement is also computationally very efficient. Future research will involve adapting both these techniques for the problem of simulating time-evolving turbulence.

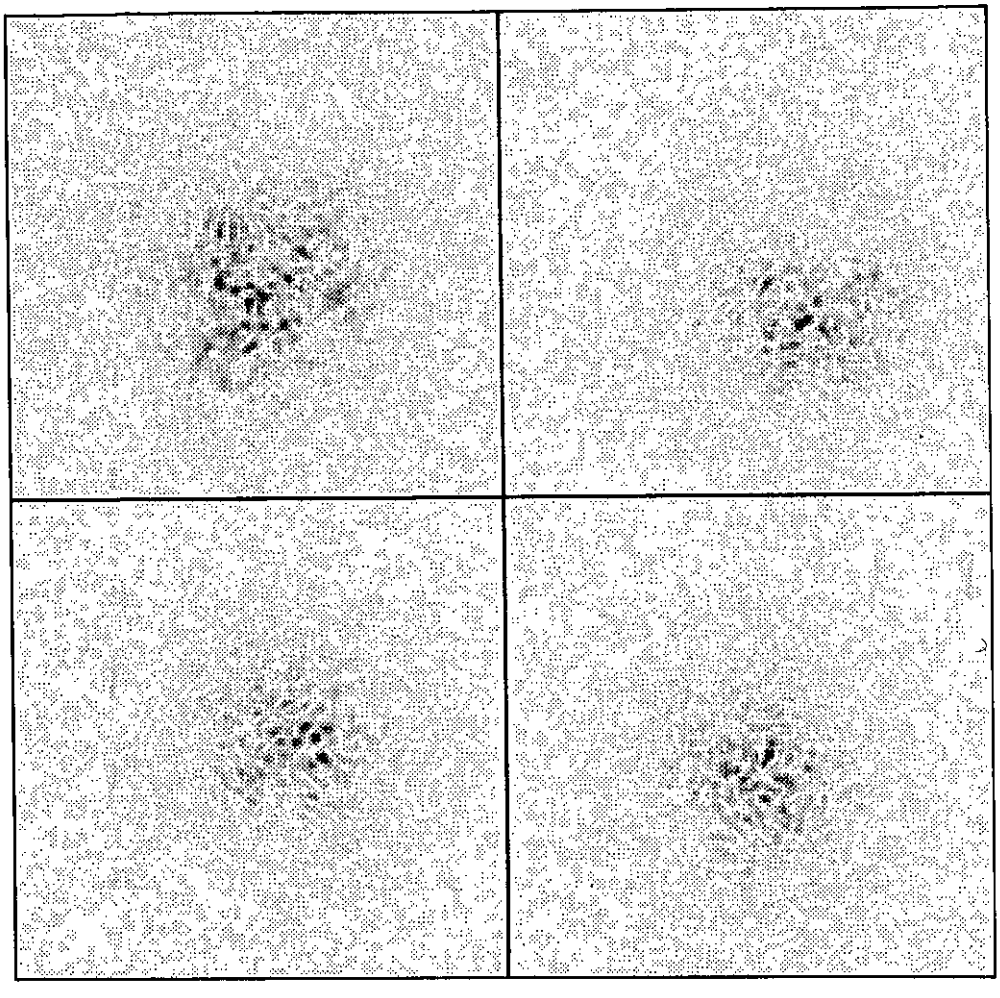

Figure 11. Typical speckle images produced by the fractal simulation.

Acknowledgments

This work was supported under SERC research grants GR/F13478 and GR/F75544. AG would like to thank the Deutsche Forschungsgemeinschaft for financial support.

References

[1] Roddier F 1981 The Effects of Atmospheric Turbulence in Optical Astronomy *Progress in Optics 19* ed E Wolf (Amsterdam: North Holland) 281–376

[2] Fried D L 1965 Statistics of a geometric representation of wavefront distortion *J. Opt. Soc. Am.* **55** 1427–35

[3] Noll R J 1976 Zernike polynomials and atmospheric turbulence *J. Opt. Soc. Am.* A **66** 207–11

[4] Bracewell R N 1986 *The Fourier Transform and its Applications* 2nd edn (New York: McGraw–Hill)

[5] Roddier N 1990 Atmospheric wavefront simulation using Zernike polynomials *Opt. Eng.* **29** 1174–80

[6] Peitgen H O and Saupe D (eds) 1988 *The Science of Fractal Images* (London: Springer–Verlag)

[7] Shaklan S B Multiple beam correlation using single-mode fiber optics with application to interferometric imaging *PhD Thesis* University of Arizona

[8] Rabiner L R and Gold B 1975 *Theory and Application of Digital Signal Processing* (Englewood Cliffs, NJ: Prentice Hall)

[9] McGlamery B L 1976 Computer simulation studies of compensation of turbulence degraded images *SPIE/OSA Proc.* **74** 225–33

[10] Mandelbrot B B 1982 Comment on the computer rendering of fractal stochastic models *Commun. ACM* **25** 581–3

[11] Fournier A, Fussell D and Carpenter L 1982 Computer rendering of stochastic models *Commun. ACM* **25**